

STR genetic diversity from the Human Genome Diversity Project (HGDP) populations.

Tamara Soledad Frontanilla^{a*}, Guilherme Valle-Silva^b, Jesús Ayala^c, Celso Teixeira Mendes-Junior^a.

^aDepartamento de Genética, Faculdade de Medicina de Ribeirão Preto, Universidade de São Paulo, 14049-900, Ribeirão Preto, SP, Brazil.

^bDepartamento de Química, Laboratório de Pesquisas Forenses e Genômicas, Faculdade de Filosofia, Ciências e Letras de Ribeirão Preto, Universidade de São Paulo, 14040-901, Ribeirão Preto, SP, Brazil.

^cUniversidad de la Integración de las Americas. Asunción, Paraguay.

*Corresponding author:

Tamara Soledad Frontanilla
tfronta@gmail.com

ORCID ID

Tamara Soledad Frontanilla: 0000-0002-6873-7813

Guilherme Valle-Silva: 0000-0002-0062-9162

Jesus Ayala: 0000-0002-7065-6879

Celso Teixeira Mendes-Junior: 0000-0002-7337-1203

1 **ABSTRACT**
2

3 The Human Genome Diversity Project (HGDP) studied 54 worldwide
4 populations comprising seven population groups: African, American, Central
5 South Asian, East Asian, European, Middle Eastern, and Oceanian. This study
6 aimed to perform a comprehensive genotyping analysis of STRs commonly used
7 in forensic and population genetic studies from the Human Genome Diversity
8 Project dataset and to publish it as an open-access STR database to contribute
9 to future forensic genetics studies. A set of 22 STR markers were analyzed using
10 high-coverage Whole-Genome Sequencing data from BAM files available at the
11 International Genome Sample Resource. HipSTR was used to call genotypes
12 from 929 samples from all 54 population samples. To validate our results, we
13 directly compared our NGS-based and CE-based genotypes on 16 STRs
14 available in Rosenberg lab (Stanford University) dataset. Also, the allele
15 frequencies estimated were compared with the data stored at the SPSmart STR
16 browser. Forensic parameters, allele frequencies, and Hardy-Weinberg
17 equilibrium adherence were calculated for each population. Principal Coordinate
18 Analysis (PCoA), the Analysis of Molecular Variance (AMOVA), and clustering
19 analysis were used to evaluate population structure. The D21S11 marker could
20 not be detected in the present study. The average successful calling rate was
21 90.27%, ranging from 58.56% (Penta D) to 97.85% (D3S1358). Comparing both
22 databases, the average number of identical genotypes was 97.44%. In
23 conclusion, this investigation offers a population genetics perspective based on
24 a comprehensive genotyping analysis of STR commonly used in the forensic
25 genetics field, concerning the whole Human Genome Diversity Project dataset.
26 Except for Penta D and Penta E, all genotypes and allele frequencies presented
27 in this study are supported by (a) previous reports that certify HipSTR's reliability,
28 (b) the comparison between CE-derived and NGS-derived genotypes, (c)
29 frequency data reports from worldwide populations, including the large popSTR
30 database, and (d) the conclusions achieved by our population genetics analysis
31 that corroborates current knowledge regarding modern human demographic
32 history.

33 **Keywords:** HipSTR; allele frequencies; forensic genetics; worldwide population;
34 bioinformatics.

35 **INTRODUCTION**
36

37 The Human Genome Diversity Project (Almarri et al., 2020; Bergström et
38 al., 2020; Cavalli-Sforza, 2005) (HGDP) is a collaboration of scientists worldwide
39 to create a database of different world populations. It was started in 1990 by
40 Stanford University's Morrison Institute (Cann et al., 2022; Rosenberg, 2006).
41 The project initially had some ethical issues concerning indigenous populations
42 (Dodson et al., 1999), who are considered vulnerable and might be exploited
43 (Cavalli-sforza, 2005). In 1994, after a few years of discussion, the US National
44 Research Council (NRC) of the National Academy of Sciences (NAS)
45 recommended that the HGDP should proceed because of the countless scientific
46 benefits, but always carrying out the necessary care and consent. This project
47 studied 54 worldwide populations comprising seven population groups: African,
48 American, Central South Asian, East Asian, European, Middle Eastern, and
49 Oceanian (Bergström et al., 2020).

50 There are many international collaborative genome-wide studies, such as
51 The Human Genome Project (HGP) (Birney, 2021) the Haplotype Map (HapMap)
52 project (1000 Genomes Project Consortium et al., 2015), the Human Genome
53 Diversity Project (Cavalli-Sforza, 2005), and the 1000 Genomes Project (1000
54 Genomes Project Consortium et al., 2015). The first two focus on mapping and
55 sequencing genes to discover their relationship with different diseases. However,
56 the HGDP and the 1000 Genomes Project are more interested in understanding
57 the extent of genetic variation between humans. Although The 1000 Genomes
58 Project has produced an extensive catalog of human genetic variation, the HGDP
59 contains samples of underrepresented human populations or isolated indigenous
60 populations that are necessary to better understand the demographic history and
61 introgression of Neanderthals and Denisovans' DNA into modern human
62 genomes (Callaway, 2019; Degioanni et al., 2019; Demeter et al., 2022).

63 Next generation sequencing (NGS) (Behjati et al., 2013), also known as
64 massively parallel sequencing or deep sequencing, is a revolutionary technology
65 that allows the sequencing of millions of small DNA fragments in parallel.
66 Specifically developed bioinformatics tools are used to piece together these
67 fragments using the human reference genome as a backbone. NGS can evaluate

68 thousands or even millions of *loci* simultaneously compared with just a few dozen
69 *loci* detected by PCR and electrophoresis (Bonneville *et al.*, 2020).

70 Genome-wide studies, including exome and/or whole-genome
71 sequencing, are becoming more and more common worldwide for diagnosing
72 rare genetic diseases and predicting possible forthcoming conditions. Such
73 datasets allow for the analysis of more complex genetic regions that are usually
74 left aside, such as Short Tandem Repeats (STR) markers. STRs are composed
75 of consecutive repetitive units of 2-6 base pairs that form series with lengths of
76 up to 100 nucleotides or even more (Fan; 2007). Typically, capillary
77 electrophoresis (CE) is the technique used to genotype these markers after PCR
78 amplification. However, recent articles (Ganschow *et al.*, 2018; Gymrek *et al.*,
79 2012; Valle-Silva *et al.*, 2022; Warshauer *et al.*, 2013; Willems *et al.*, 2017)
80 showed that specific bioinformatic tools could successfully genotype these
81 markers from NGS data.

82 Haplotype inference and phasing for STRs (Willems *et al.*, 2017; Gordon
83 *et al.*, 2017) (HipSTR) is a bioinformatic tool developed for calling STR markers
84 specifically from Whole Genome Sequencing (WGS). It was created to process
85 hundreds of samples at once, making it suitable to deal with large databases.
86 Moreover, HipSTR learns locus-specific PCR stutter models using an EM
87 algorithm, employing a specialized hidden Markov model to align reads to
88 candidate alleles while accounting for STR artifacts and using phased SNP
89 haplotypes to genotype and phase STR. HipSTR showed high accuracy in
90 previous studies, demonstrating a 98.8% consistency compared with capillary
91 electrophoresis in 118 samples (Halman; Oshlack, 2020). Valle-Silva *et al.* (2022)
92 compared three software to genotype STR markers from NGS data showing
93 more than 97% calling accuracy between them.

94 This study aimed to perform a comprehensive genotyping analysis of
95 STRs commonly used in population genetics studies from the Human Genome
96 Diversity Project dataset and to publish it as an open-access STR database.

97
98

99 **METHODOLOGY**100
101 **Genotype Calling**

102

103 The population sample consisted of 929 individuals from the Human
 104 Genome Diversity Project (HGDP) panel, distributed across 54 worldwide
 105 populations that compose seven population groups: Africa ($n=104$), Americas
 106 ($n=61$), Central South Asia ($n=197$), East Asia ($n=223$), Europe ($n=155$), Middle
 107 East ($n=161$) and Oceania ($n=28$). These populations are described by
 108 Bergstrom et al. (Bergström et al., 2020) (Table 1). The CRAM files containing
 109 sequence data from these 929 samples are available at the International Genome
 110 Sample Resource, divided into two datasets: one presented by Mallick et al.
 111 (Mallick et al., 2016) (<https://www.internationalgenome.org/data-portal/data-collection/hgdp>), and the other by Bergström et al. (2020)
 112 (<https://www.internationalgenome.org/data-portal/data-collection/sgdp>).

114

115 **Table 1. Population samples from the Human Genome Diversity Project**
 116 **(HGDP) used in this study ($n=929$).**

117

Population	Subpopulation	Nomenclature	Number of individuals
Africa	BantuKenya	AFR001	11
	BantuSouthAfrica	AFR002	8
	Biaka	AFR003	22
	Mandenka	AFR004	22
	Mbuti	AFR005	13
	San	AFR006	6
America (Amerindians)	Yoruba	AFR007	22
	Colombian	AMR008	7
	Karitia	AMR009	12
	Maya	AMR010	21
	Pima	AMR011	13
Central/South Asia	Surui	AMR012	8
	Balochi	CSA013	24
	Brahui	CSA014	25
	Burusho	CSA015	24
	Hazara	CSA016	19
	Kalash	CSA017	22
	Makrani	CSA018	25
	Pathan	CSA019	24
	Sindhi	CSA020	24

	Uygur	CSA021	10
East Asia	Oxi	EAS022	8
	Cambodian	EAS023	9
	Dai	EAS024	9
	Daur	EAS025	9
	Han	EAS026	33
	Hezhen	EAS027	9
	Japanese	EAS028	27
	Lahu	EAS029	8
	Miao	EAS030	10
	Mongolian	EAS031	9
	NorthernHan	EAS032	10
	Oroqen	EAS033	9
	She	EAS034	10
	Tu	EAS035	10
Europe	Tujia	EAS036	9
	Xibo	EAS037	9
	Yakut	EAS038	25
	Yi	EAS039	10
	Adygei	EUR040	16
	Basque	EUR041	23
	Bergamoltalian	EUR042	12
	French	EUR043	28
Middle East	Orcadian	EUR044	15
	Russian	EUR045	25
	Sardinian	EUR046	28
	Tuscan	EUR047	8
	Bedouin	MES048	46
	Druze	MES049	42
	Mozabite	MES050	27
Oceania	Palestinian	MES051	46
	Bougainville	OCE052	11
	PapuanHighlands	OCE053	9
	PapuanSepik	OCE054	8

118

119

120 All samples were sequenced in high-coverage as described by Mallick et

121 al. (MALLICK; LI; LIPSON; MATHIESON *et al.*, 2016) and Bergström et al.

122 (2020). This coverage depth provides a reliable opportunity to genotype STR

123 markers accurately despite their large sizes (i.e., repetitive sequences

124 encompassing up to 130 bp).

125 A total of 22 *loci* commonly referenced in forensic practice were analyzed:
126 CSF1PO, D1S1656, D2S441, D2S1338, D3S1358, D5S818, D7S820, D8S1179,
127 D10S1248, D12S391, D13S317, D16S539, D18S51, D19S433, D21S11,
128 D22S1045, FGA, Penta D, Penta E, TH01, TPOX, and vWA. The HipSTR
129 (Willems et al., 2017) algorithm was run for each individual to genotype the 22
130 STRs based on the human reference genome GRCh38, and using the BED file
131 hg38.hipstr_reference.bed with the flanking regions available in the HipSTR
132 repository (<https://github.com/HipSTR-Tool/HipSTR-references/>). A minimum of
133 8 reads were accepted to obtain reliable genotypes, and the 15% stutter model
134 as a calling filter was used.

135 The genotypes for each marker were calculated using three parameters
136 provided in the output VCF file: the reference allele of each marker, the period
137 (i.e., the length of each STR repeat unit), and the base pair differences (GB) in
138 comparison with the reference allele (Willems et al., 2017). Nomenclature
139 adjustments were made for D19S433, Penta D, Penta E, and vWA following
140 Valle-Silva et al. (Valle-Silva et al., 2022) recommendations to couple with the
141 nomenclature established by the International Society for Forensic Genetics
142 (ISFG) (Gettings; et al., 2019). By using the IGV software (Robinson et al., 2017;
143 Thorvaldsdóttir et al., 2013) and the HipSTR VizAIn function (Willems et al.,
144 2017), we have previously demonstrated that the alleles provided by HipSTR for
145 these four markers (D19S433, Penta D, Penta E, and vWA) needed
146 nomenclature adjustment to avoid a shift of some base pairs in allele calling
147 (Valle-Silva et al., 2022). The adjustments consisted of removing two repeat units
148 from all D19S433 and vWA alleles called by HipSTR, including one repeat unit
149 into all Penta D alleles, and removing two nucleotides from all Penta E alleles
150 (Gettings et al., 2019).

151
152 **Statistical Analysis**

153
154 Forensic parameters [Match Probability (MP), Power of Discrimination
155 (PD), Power of Exclusion (PE), and Polymorphism Information Content (PIC)],
156 allele frequencies, and Hardy-Weinberg equilibrium adherence were estimated
157 for each population group using GenAIEx 6.5 (Peakall, 2012) and STRAF 2.5.1
158 software (Gouy; Zieger, 2017).

159 To explore the distribution of genetic diversity across populations of
160 different ethnic backgrounds, the Principal Coordinate Analysis (PCoA), the
161 Analysis of Molecular Variance (AMOVA), and clustering analysis were done
162 using GenAIEx 6.5 (Peakall, 2012), Arlequin 3.5 (Excoffier; Lischer, 2010), and
163 STRUCTURE 2.3.4 (Hubisz et al., 2009) software, respectively. The
164 STRUCTURE analysis was performed for k ranging from 3 to 7, applying the
165 correlated allele frequency model and 200.000 burn-in steps followed by 200.000
166 Markov Chain Monte Carlo interactions in 10 independent runs. The results from
167 the runs with the largest “Estimated Ln Probability of Data” [LnP(D)] were
168 selected and are depicted in bar plots created with Clumpak (Kopelman et al.,
169 2015).

170

171 **Genotype validation**

172

173 We used two validation methodologies to verify the reliability of genotype
174 data generated by HipSTR. The first one consisted of a direct comparison with
175 CE-derived genotypes available in the Rosenberg's lab (Stanford University)
176 dataset available at:
177 <https://rosenberglab.stanford.edu/data/algeeheittEtAl2016/HGDPmicrosatsIncludinCODIS.stru>. The dataset is composed of the data published by Algee-
178 Hewitt et al. (2016) (Algee-Hewitt et al., 2016) and Rosenberg et al. (2005)
179 (Rosenberg et al., 2005). We used 865 individuals and 16 STR markers present
180 in both the NGS and CE datasets for this validation.

182 In a secondary validation attempt, the allele frequencies estimated in the
183 present study were compared with allele frequency data from the same seven
184 major population groups (African, European, Middle Eastern, Central South
185 Asian, East Asian, Oceanian, and American) stored at the SPSmart STR browser
186 (Amigo et al., 2009; Fernandez et al., 2009) (Pop.STR). For this comparison,
187 pairwise F_{ST} was estimated using the Arlequin software (Excoffier; Lischer, 2010).

188

189 **RESULTS**

190

191 STR genotypes established for each individual from the HGDP dataset using
192 HipSTR are available in Supplementary Table 1 as an open-access database.
193 The D21S11 marker was excluded because we failed in genotyping it. The mean

194 coverage for genotype calling ranged from 29.765 (Penta D) to 53.869
195 (D3S1358) (Table 2).

196 Table 3 shows the allele frequencies and forensic parameters for the whole
197 HGDP dataset, while Supplementary Table 2 presents these same parameters
198 for each of the seven major population groups studied. The average successful
199 calling rate was 90.27%, ranging from 58.56% (Penta D) to 97.85% (D3S1358)
200 (Table 3). HipSTR failed in genotyping the Penta D alleles smaller than five
201 repeats. Moreover, Penta E was in H-W disequilibrium in half (27) of the 54
202 population samples (Table 4). Thus, these markers were excluded from all
203 interpopulation statistical analyses performed in the present study (Analysis of
204 Molecular Variance, STRUCTURE analysis, and PCoA). It is noteworthy that the
205 D22S1045 was monomorphic in a small ($n=13$) Amerindian population sample of
206 Mexico (Pima); however, this is due to a lack of genetic diversity in this locus
207 rather than genotyping errors.

208 **Table 2. Average coverages obtained for each STR using the HipSTR tool.**
209

Marker	Lowest value	Median	Highest value	Mean	Standard deviation
CSF1PO	22	47	158	47.704	14.659
D1S1656	21	49	138	49.757	15.574
D2S441	19	48	125	48.643	14.656
D2S1338	28	52	115	47.994	22.810
D3S1358	23	53	134	53.869	15.041
D5S818	12	44	117	44.856	13.887
D7S820	18	41	118	41.309	12.603
D8S1179	24	50	137	50.962	15.589
D10S1248	20	43	105	43.073	14.102
D12S391	23	53	122	48.841	22.612
D13S317	15	40	120	40.670	13.406
D16S539	25	48	123	47.867	14.269
D18S51	29	52	154	50.016	22.480
D19S433	22	47	104	45.073	16.933
D22S1045	8	46	121	39.821	22.946
FGA	28	56	132	50.909	23.812
PentaD	16	38	130	29.765	27.295
PentaE	11	39	119	30.427	23.215
TH01	17	40	115	40.778	12.295
TPOX	19	37	101	35.364	14.620
vWA	23	44	173	43.086	22.804

210

211 **Table 3. Allele frequencies and the forensic parameters estimated for each marker in the whole HGDP dataset.**

212

Allele	CSF1PO	D1S1656	D2S441	D2S1338	D3S1358	D5S818	D7S820	D8S1179	D10S1248	D12S391	D13S317	D16S539	D18S51	D19S433	D22S1045	FGA	PentaD	PentaE	TH01	TPOX	vWA					
5																	0.002	0.100								
5.2																0.001										
6	0.001							0.001										0.007		0.204	0.012					
7	0.010							0.019	0.018		0.001							0.014	0.108	0.237	0.006					
8	0.012	0.003	0.001					0.014	0.167	0.006	0.002							0.040	0.053	0.141	0.457					
9	0.024	0.002	0.003					0.055	0.086	0.005	0.001					0.099	0.172		0.001		0.252	0.036	0.265	0.135		
9.1								0.005			0.001															
9.3								0.001														0.133				
10	0.261	0.006	0.215					0.132	0.256	0.110	0.001					0.087	0.116	0.005	0.014	0.014		0.165	0.085	0.018	0.076	
10.1																0.001										
10.3																0.001										
11	0.275	0.071	0.351					0.314	0.277	0.063	0.008					0.269	0.291	0.014	0.012	0.179		0.194	0.232	0.002	0.276	0.001
11.1											0.001															
11.2																	0.001	0.001								
11.3								0.056																		
11.4																						0.001				
12	0.356	0.085	0.087					0.001	0.288	0.162	0.117	0.052				0.284	0.262	0.087	0.072	0.018		0.132	0.205	0.001	0.038	
12.1																	0.001									
12.2																	0.001	0.008								
12.3								0.009									0.001									
13	0.054	0.095	0.032					0.003	0.163	0.030	0.235	0.258				0.084	0.125	0.128	0.259	0.005		0.134	0.088		0.001	
13.1																	0.001									
13.2																	0.002	0.044								
13.3								0.001	0.002																	
14	0.006	0.117	0.211					0.057	0.014	0.003	0.238	0.296	0.001	0.026	0.018	0.181	0.286	0.046		0.040	0.057			0.131		
14.2																	0.060									
14.3								0.002																		
15	0.001	0.183	0.023					0.351	0.001		0.166	0.223	0.022	0.001	0.002	0.157	0.093	0.326		0.009	0.029			0.087		
15.2																	0.089									

15.3	0.021																		
16	0.185	0.003	0.027	0.284	0.001	0.048	0.124	0.023		0.121	0.035	0.251	0.001	0.007	0.006			0.230	
16.2				0.001						0.001	0.023								
16.3	0.043																		
17	0.064	0.001	0.138	0.201		0.011	0.033	0.092		0.126	0.001	0.154	0.001	0.002				0.268	
17.1								0.001											
17.2										0.001									
17.3	0.080							0.008											
18	0.011		0.081	0.094		0.002	0.002	0.210		0.089		0.007	0.012					0.188	
18.2										0.001			0.001						
18.3	0.023							0.016											
19			0.163	0.009				0.205		0.051		0.001	0.053					0.078	
19.1								0.001											
19.2								0.001					0.002						
19.3	0.008							0.006											
20			0.136					0.141		0.021			0.078					0.014	
20.2													0.001						
21			0.036					0.099		0.010			0.122					0.001	
21.2													0.003						
22			0.053					0.081		0.004			0.219						
22.2													0.005						
22.3								0.001											
23			0.226					0.056		0.001			0.158						
23.2													0.004						
24			0.086					0.027		0.001			0.178						
24.2									0.001				0.003						
24.3													0.001						
25			0.045					0.007					0.102						
25.2													0.004						
26			0.009					0.001					0.041						
26.2								0.001						0.008					
27																			

28

28.1

30

0.004

0.001

0.001

	CSF1PO	D1S1656	D2S441	D2S1338	D3S1358	D5S818	D7S820	D8S1179	D10S1248	D12S391	D13S317	D16S539	D18S51	D19S433	D22S1045	FGA	PentaD	PentaE	TH01	TPOX	vWA
N	905	903	908	793	909	907	907	903	886	806	899	902	823	852	778	800	544	627	905	850	803
Na	10	18	16	11	9	10	11	11	13	22	9	9	20	19	10	24	13	12	8	7	10
Ho	0.728	0.843	0.675	0.755	0.724	0.731	0.763	0.792	0.721	0.814	0.750	0.763	0.854	0.764	0.666	0.754	0.778	0.440	0.706	0.664	0.762
He	0.726	0.883	0.773	0.864	0.744	0.770	0.795	0.829	0.777	0.864	0.800	0.787	0.877	0.822	0.773	0.860	0.832	0.859	0.794	0.689	0.808
MP	0.126	0.025	0.081	0.037	0.109	0.085	0.071	0.051	0.081	0.033	0.068	0.076	0.028	0.053	0.087	0.036	0.050	0.058	0.070	0.151	0.062
PE	0.473	0.681	0.391	0.519	0.466	0.478	0.532	0.584	0.462	0.625	0.509	0.532	0.703	0.534	0.377	0.516	0.558	0.140	0.438	0.374	0.531
PD	0.874	0.975	0.919	0.963	0.891	0.915	0.929	0.949	0.919	0.967	0.932	0.924	0.972	0.947	0.913	0.964	0.950	0.942	0.930	0.849	0.938
PIC	0.677	0.873	0.741	0.850	0.702	0.735	0.765	0.807	0.742	0.850	0.772	0.755	0.864	0.801	0.738	0.844	0.811	0.845	0.762	0.642	0.781
CMP	3.72.E-26																				
CPE	0.999999676																				

213 N: number of samples; Na: number of alleles; Ho: Observed Heterozygosity; He: Expected Heterozygosity; MP: match probability; PE: power of exclusion; PD:
214 power of discrimination; PIC: polymorphism information content; CMP: combined match probability; CPE combined power of exclusion.
215
216
217
218
219
220
221
222
223
224
225
226
227
228
229
230
231

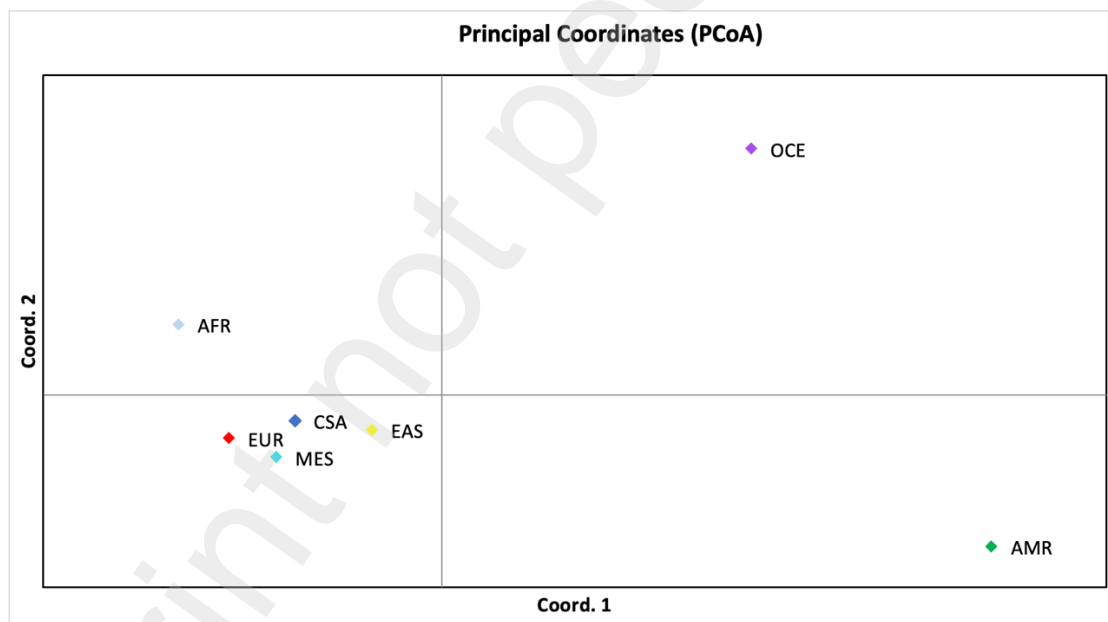
232 **Table 4. Probabilities of adherence to Hardy-Weinberg equilibrium proportions for each STR in all 54 subpopulations analyzed in the**
 233 **HGDP. Significant p-values ($\alpha = 0.05$) are in boldface.**
 234

Pop	CSF1PO	D1S1656	D2S441	D2S1338	D3S1358	D5S818	D7S820	D8S1179	D10S1248	D12S391	D13S317	D16S539	D18S51	D19S433	D22S1045	FGA	PentaD	PentaE	TH01	TPOX	vWA
AFR001	0.539	0.248	0.766	0.628	0.673	0.433	0.763	0.988	0.290	0.174	0.837	0.300	0.521	0.682	0.340	0.223	0.423	0.336	0.191	0.505	0.842
AFR002	0.712	0.350	0.824	0.229	0.824	0.930	0.440	0.621	0.374	0.888	0.273	0.261	0.438	0.161	0.017	0.177	0.157	0.116	0.673	0.704	0.390
AFR003	0.074	0.812	0.008	0.636	0.181	0.537	0.529	0.900	0.947	0.379	0.808	0.929	0.562	0.363	0.042	0.787	0.450	0.059	0.553	0.834	0.985
AFR004	0.742	0.461	0.662	0.201	0.916	0.967	0.576	0.630	0.964	0.441	0.724	0.648	0.141	0.992	0.245	0.864	0.526	0.004	0.702	0.136	0.603
AFR005	0.207	0.256	0.085	0.012	0.617	0.938	0.519	0.427	0.669	0.751	0.631	0.518	0.289	0.353	0.256	0.121	0.823	0.038	0.569	0.607	0.900
AFR006	0.556	0.548	0.227	0.654	0.868	0.678	0.556	0.868	0.166	0.874	0.054	0.226	0.174	0.626	0.767	0.062	0.766	0.207	0.995	0.502	0.393
AFR007	0.291	0.317	0.981	0.305	0.059	0.011	0.381	0.289	0.605	0.385	0.425	0.257	0.812	0.631	0.708	0.283	0.595	0.007	0.682	0.149	0.561
AMR008	0.914	0.678	0.914	0.694	0.466	0.950	0.312	0.556	0.021	0.735	0.479	0.776	0.511	0.575	0.034	0.282	0.387	0.116	0.626	0.152	0.626
AMR009	0.122	0.724	0.197	0.308	0.785	0.942	0.950	0.711	0.615	0.535	0.044	0.568	0.031	0.763	0.451	0.820	0.841	0.083	0.376	0.792	0.043
AMR010	0.999	0.446	0.990	0.687	0.524	0.254	0.707	0.403	0.461	0.001	0.283	0.795	0.149	0.210	0.011	0.138	0.678	0.008	0.795	0.463	0.566
AMR011	0.800	0.645	0.199	0.461	0.637	0.001	0.229	0.853	0.337	0.949	0.307	0.615	0.460	0.200	-	0.546	0.711	0.003	0.623	0.028	0.827
AMR012	0.820	0.498	0.686	0.978	0.983	0.028	0.719	0.836	0.726	0.557	0.947	0.217	0.545	0.117	0.054	0.628	0.542	0.046	0.733	0.409	0.442
CSA013	0.532	0.273	0.165	0.350	0.000	0.215	0.869	0.718	0.478	0.306	0.915	0.224	0.737	0.063	0.565	0.011	0.892	0.000	0.655	0.861	0.802
CSA014	0.909	0.407	0.073	0.334	0.010	0.809	0.973	0.688	0.920	0.870	0.588	0.735	0.620	0.106	0.557	0.329	0.363	0.614	0.325	0.726	0.845
CSA015	0.615	0.611	0.617	0.746	0.043	0.037	0.695	0.144	0.875	0.135	0.922	0.374	0.999	0.091	0.765	0.000	0.584	0.011	0.366	0.797	0.342
CSA016	0.652	0.940	0.009	0.521	0.849	0.669	0.180	0.917	0.006	0.457	0.290	0.073	0.764	0.867	0.163	0.039	0.272	0.136	0.194	0.423	0.611
CSA017	0.873	0.966	0.079	0.799	0.467	0.985	0.486	0.983	0.608	0.840	0.632	0.361	0.577	0.064	0.001	0.088	0.607	0.022	0.882	0.823	0.810
CSA018	0.759	0.565	0.997	0.920	0.442	0.847	0.876	0.645	0.320	0.030	0.154	0.249	0.733	0.192	0.221	0.596	0.248	0.001	0.912	0.949	0.343
CSA019	0.984	0.787	0.908	0.488	0.593	0.716	0.085	0.857	0.465	0.007	0.350	0.144	0.510	0.716	0.845	0.345	0.559	0.153	0.764	0.834	0.908
CSA020	0.976	0.585	0.797	0.792	0.436	0.707	0.124	0.689	0.939	0.930	0.795	0.168	0.191	0.107	0.937	0.485	0.081	0.001	0.955	0.461	0.684
CSA021	0.093	0.803	0.884	0.585	0.379	0.777	0.264	0.899	0.606	0.609	0.756	0.258	0.214	0.678	0.678	0.084	0.509	0.013	0.029	0.540	0.399
EAS022	0.460	0.611	0.421	0.262	0.587	0.440	0.760	0.269	0.896	0.718	0.154	0.741	0.453	0.466	0.570	0.505	0.396	0.019	0.311	0.572	0.212
EAS023	0.779	0.917	0.173	0.732	0.231	0.543	0.676	0.493	0.656	0.779	0.511	0.523	0.469	0.902	0.516	0.245	0.744	0.109	0.103	0.895	0.521
EAS024	0.213	0.607	0.182	0.006	0.948	0.134	0.544	0.101	0.947	0.866	0.685	0.467	0.233	0.172	0.320	0.899	0.849	0.003	0.837	0.896	0.744
EAS025	0.083	0.621	0.423	0.656	0.878	0.197	0.016	0.009	0.620	0.326	0.137	0.276	0.482	0.312	0.320	0.388	0.338	0.006	0.586	0.322	0.815
EAS026	0.930	0.823	0.831	0.868	0.960	0.693	0.569	0.727	0.121	0.239	0.920	0.025	0.989	0.961	0.610	0.540	0.562	0.000	0.587	0.867	0.829
EAS027	0.677	0.103	0.969	0.373	0.652	0.794	0.479	0.577	0.183	0.413	0.206	0.524	0.932	0.661	0.720	0.704	0.804	0.229	0.099	0.726	0.518
EAS028	0.712	0.008	0.215	0.815	0.481	0.792	0.243	0.257	0.690	0.988	0.674	0.649	0.301	0.404	0.850	0.928	0.373	0.000	0.223	0.623	0.622

EAS029	0.631	0.572	0.423	0.651	0.947	0.777	0.850	0.820	0.478	0.725	0.389	0.147	0.739	0.353	0.796	0.649	0.641	0.132	0.824	0.685	0.226
EAS030	0.374	0.839	0.345	0.354	0.019	0.567	0.714	0.452	0.317	0.432	0.695	0.832	0.247	0.922	0.538	0.469	0.540	0.256	0.329	0.606	0.738
EAS031	0.376	0.967	0.799	0.641	0.638	0.878	0.922	0.223	0.895	0.529	0.734	0.575	0.168	0.676	0.572	0.375	0.891	0.062	0.941	0.789	0.761
EAS032	0.202	0.581	0.571	0.192	0.398	0.704	0.288	0.198	0.717	0.418	0.548	0.595	0.154	0.332	0.815	0.956	0.870	0.103	0.497	0.111	0.402
EAS033	0.791	0.389	0.268	0.626	0.599	0.387	0.895	0.789	0.615	0.602	0.639	0.877	0.252	0.120	0.581	0.459	0.936	0.022	0.806	0.946	0.465
EAS034	0.546	0.287	0.363	0.440	0.506	0.481	0.375	0.787	0.974	0.966	0.800	0.925	0.582	0.538	0.274	0.258	0.507	0.177	0.374	0.120	0.570
EAS035	0.681	0.413	0.590	0.637	0.379	0.427	0.537	0.924	0.611	0.497	0.453	0.050	0.816	0.431	0.799	0.459	0.711	0.227	0.501	0.587	0.534
EAS036	0.119	0.171	0.369	0.402	0.656	0.685	0.544	0.956	0.855	0.804	0.402	0.922	0.854	0.232	0.366	0.451	0.677	0.125	0.723	0.472	0.370
EAS037	0.265	0.276	0.342	0.412	0.532	0.509	0.187	0.077	0.812	0.442	0.752	0.382	0.279	0.768	0.544	0.078	0.716	0.282	0.552	0.716	0.891
EAS038	0.977	0.005	0.801	0.400	0.928	0.902	0.924	0.354	0.951	0.942	0.871	0.592	0.966	0.964	0.238	0.791	0.646	0.215	0.768	0.849	0.866
EAS039	0.769	0.354	0.564	0.003	0.393	0.617	0.798	0.617	0.581	0.147	0.883	0.273	0.879	0.163	0.154	0.615	0.134	0.062	0.064	0.856	0.780
EUR040	0.641	0.462	0.385	0.918	0.369	0.487	0.564	0.235	0.804	0.796	0.983	0.953	0.168	0.917	0.016	0.488	0.658	0.002	0.430	0.084	0.793
EUR041	0.440	0.326	0.469	0.743	0.563	0.033	0.727	0.722	0.841	0.705	0.253	0.800	0.472	0.810	0.988	0.140	0.593	0.118	0.606	0.941	0.735
EUR042	0.091	0.073	0.292	0.376	0.434	0.470	0.005	0.218	0.851	0.525	0.026	0.512	0.689	0.540	0.907	0.221	0.220	0.032	0.216	0.625	0.245
EUR043	0.730	0.709	0.153	0.341	0.305	0.970	0.100	0.809	0.920	0.049	0.139	0.653	0.833	0.001	0.089	0.839	0.214	0.053	0.936	0.655	0.671
EUR044	0.005	0.396	0.607	0.413	0.093	0.258	0.045	0.772	0.833	0.666	0.080	0.966	0.170	0.950	0.966	0.721	0.402	0.038	0.345	0.425	0.086
EUR045	0.774	0.312	0.732	0.018	0.889	0.432	0.747	0.304	0.335	0.551	0.209	0.087	0.689	0.504	0.042	0.693	0.841	0.000	0.503	0.998	0.241
EUR046	0.515	0.137	0.065	0.728	0.530	0.393	0.665	0.223	0.414	0.104	0.822	0.961	0.421	0.692	0.680	0.331	0.172	0.002	0.619	0.333	0.234
EUR047	0.792	0.496	0.307	0.227	0.977	0.340	0.834	0.326	0.878	0.569	0.735	0.502	0.550	0.104	0.436	0.177	0.371	0.086	0.848	0.949	0.851
MES048	0.145	0.890	0.061	0.068	0.907	0.008	0.364	0.840	0.511	0.021	0.440	0.635	0.256	0.238	0.753	0.009	0.944	0.000	0.781	0.519	0.641
MES049	0.144	0.000	1.000	0.270	0.230	0.864	0.689	0.000	0.484	0.000	0.618	0.976	0.226	0.374	0.006	0.232	0.377	0.000	0.115	0.085	0.282
MES050	0.342	0.566	0.241	0.851	0.667	0.230	0.478	0.123	0.865	0.462	0.990	0.648	0.081	0.948	0.714	0.499	0.556	0.021	0.728	0.050	0.685
MES051	0.973	0.024	0.276	0.628	0.950	0.921	0.005	0.357	0.954	0.987	0.746	0.076	0.570	0.760	0.658	0.000	0.599	0.023	0.814	0.974	0.833
OCE052	0.636	0.867	0.181	0.432	0.463	0.857	0.979	0.214	0.472	0.780	0.420	0.263	0.594	0.566	0.635	0.164	0.565	0.085	0.678	0.377	0.175
OCE053	0.254	0.451	0.719	0.111	0.799	0.671	0.864	0.633	0.936	0.338	0.552	0.517	0.964	0.764	0.244	0.361	0.558	0.000	0.381	0.557	0.453
OCE054	0.849	0.154	0.686	0.674	0.974	0.062	0.272	0.276	0.647	0.160	0.183	0.412	0.371	0.916	0.108	0.164	0.729	0.157	0.757	0.677	0.867

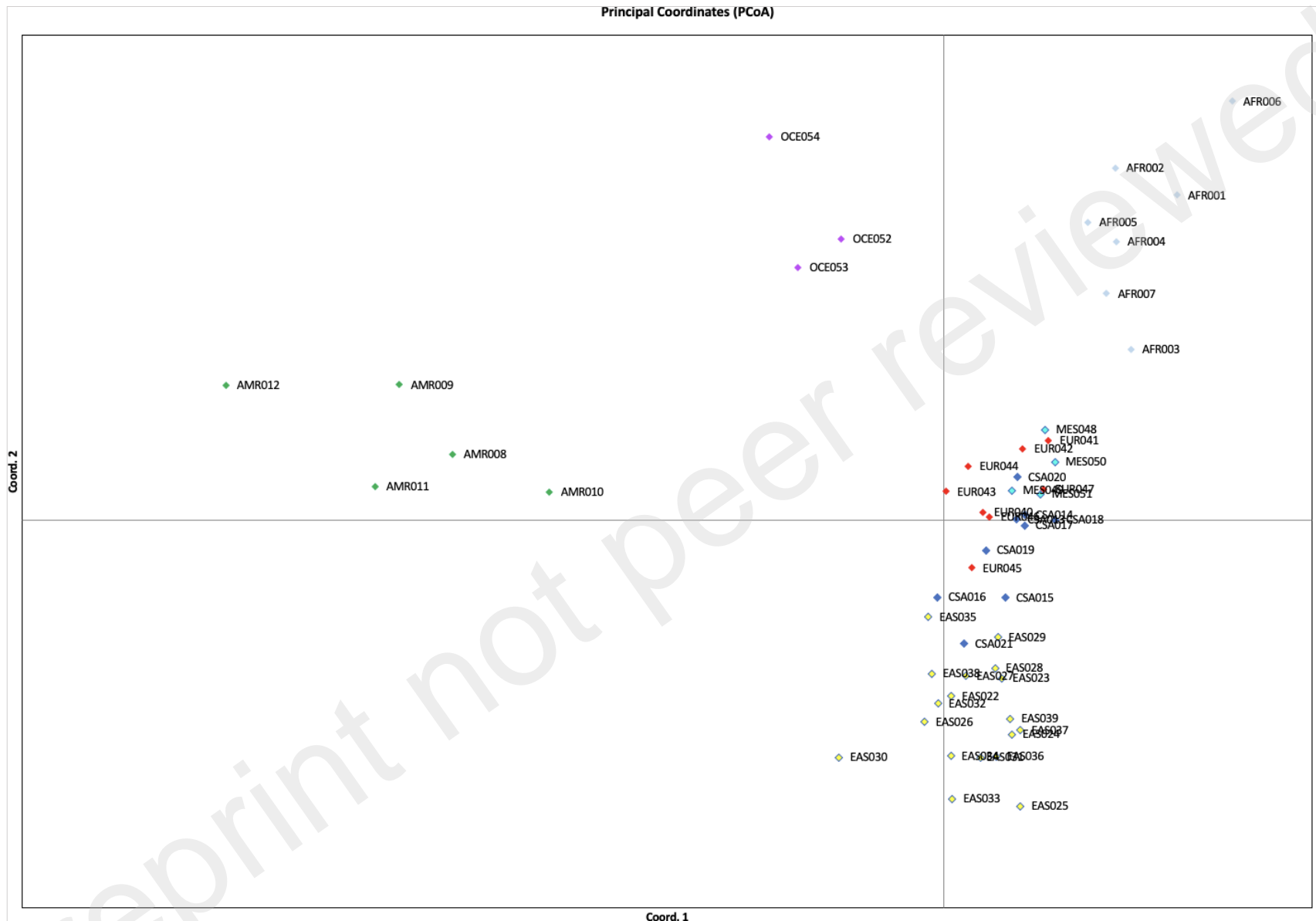
236 The Principal Coordinates Analysis (PCoA) shows a good differentiation
237 between major biogeographic populations at both continental (Figure 1) and
238 subcontinental (Figure 2) scales. For Figure 1, all subpopulations were grouped,
239 revealing four different population clusters. As expected, the African, Amerindian,
240 and Oceanian populations were placed separately (in different quadrants), while
241 the European and Asian populations were clustered together, revealing a similar
242 genetic composition. The two principal coordinates account for 70.42% of the
243 variance. In Figure 2, although the two first coordinates account for only 24.14%
244 of the variance, the distribution of the 54 subpopulations was consistent with what
245 was observed in Figure 1, resulting in four different and well-defined clusters.
246 However, in the cluster with the European and Asian populations, one may
247 observe an overlapping of populations from the four groups, mainly European,
248 Middle Eastern, and Central South Asian populations, corroborating their shared
249 ancestry and similar genetic compositions.

250



251

252 **Figure 1. Principal Coordinates Analysis (PCoA) based on autosomal STR**
253 **data from the 7 major populations of the HGDP.** Coordinates 1 and 2 account
254 for 40.66% and 29.76% of the variance, respectively. Penta D and Penta E
255 markers were excluded from this analysis. (AFR: African; CSA: Central South
256 Asia; EAS: East Asia; EUR: European; MES: Middle East; OCE: Oceania).

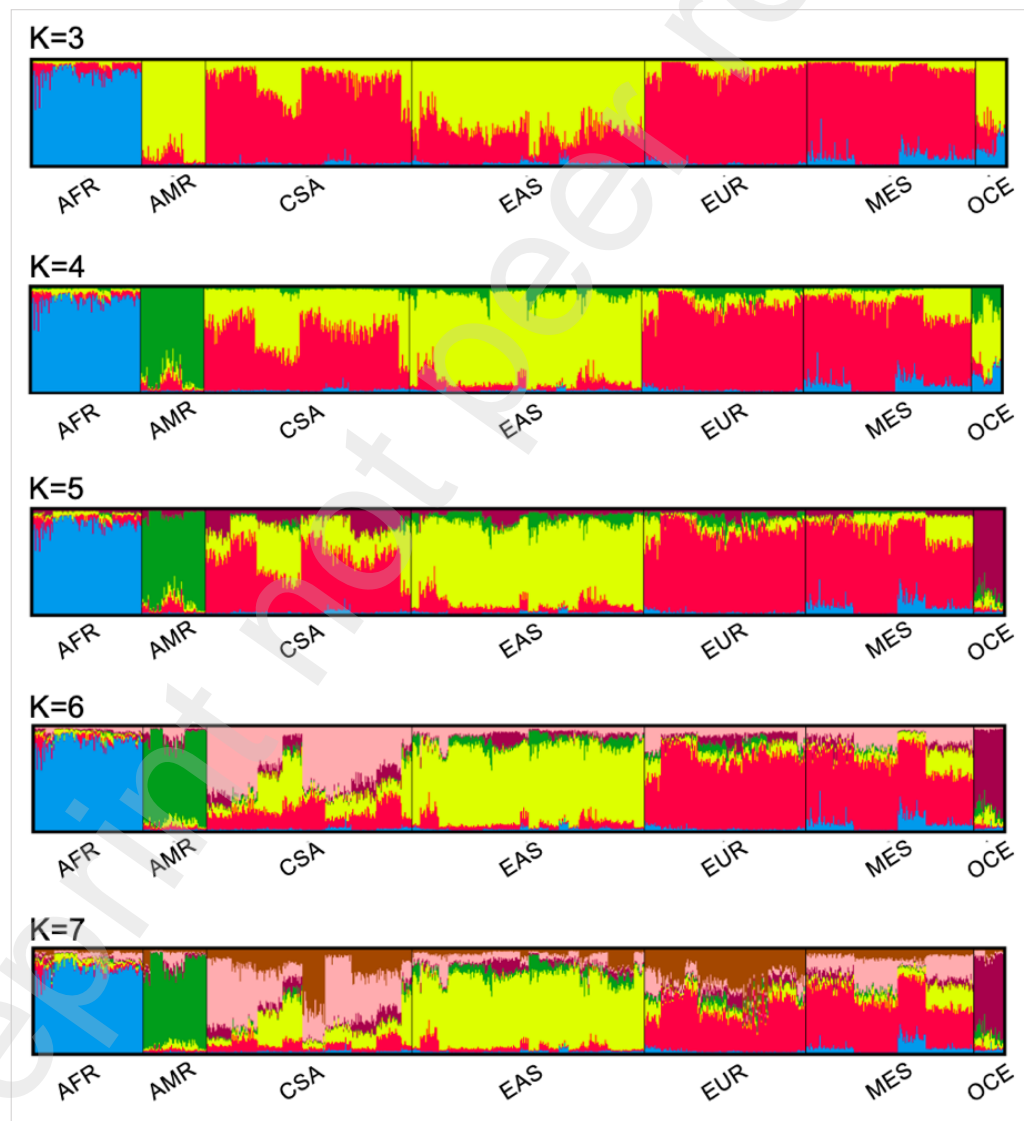


257
258
259
260

Figure 2. Principal Coordinates Analysis (PCoA) based on autosomal STR data from the 54 sub-populations of the HDGP. Coordinates 1 and 2 account for 13.48% and 10.66% of the variance, respectively. Penta D and Penta E markers were excluded from this analysis. (AFR: African; CSA: Central South Asia; EAS: East Asia; EUR: European; MES: Middle East; OCE: Oceania).

261 Similar results were obtained with the STRUCTURE analysis. Figure 3
262 depicts STRUCTURE results from runs obtained with k ranging from 3 to 7. With
263 $k = 5$, one may observe that African, Amerindian and Oceanian groups mainly
264 present their own clusters, while European and Asian populations display their
265 shared ancestry, especially European, Middle Eastern and Central South Asian
266 populations. By analyzing $k = 7$, it is possible to observe that the Central South
267 Asian populations are highly heterogeneous with each other but also present
268 evident differences when compared to European and Middle Eastern
269 populations. Although minor differences arise with $k = 7$, European and Middle
270 Eastern populations are very similar in all k .

271



272

273 **Figure 3. STRUCTURE analysis based on autosomal STR data from the 54**
274 **subpopulations of HGDP.**

275 Seven sets of 10 independent runs with the number of clusters ranging from 3 to
276 7 were conducted. Each bar plot depicts the results from the run with the largest
277 LnP(D) for the given k . Penta D and Penta E markers were excluded from this
278 analysis. (AFR: African; CSA: Central South Asia; EAS: East Asia; EUR:
279 European; MES: Middle East; OCE: Oceania).

280 To verify the distribution of variance in different levels, an AMOVA was
281 performed assuming a hierarchical structure gathering the populations in seven
282 groups: AFR, AMR, CSA, EAS, EUR, MES and OCE without the Penta E and
283 Penta D markers. Most of the variance is observed within populations (95.84%).
284 Differences between the seven groups account for 2.61% of the variance,
285 whereas only 1.55% of the variance occurs due to differences between
286 populations from the same group. An alternative structure, composed of only four
287 groups (merging CSA, EAS, EUR and MES populations in a single group),
288 revealed an increase in the variance between groups: differences between the
289 four groups account for 4.14% of the variance, whereas only 2.17% of the
290 variance occurs due to differences between populations from the same group
291 and as expected most of the variance is observed within populations (93.67%).

292 The genotypes calculated with HipSTR were compared with a dataset of
293 previously obtained CE-derived genotypes (Algee-Hewitt et al., 2016; Rosenberg
294 et al., 2005). The average number of identical genotypes was 97.44% (median =
295 99.35%) (Supplementary Table 3), ranging from 88.25% (FGA) to 99.88%
296 (D8S1179). Given the high proportion of genotypes with only one correct allele
297 for some *loci*, these figures are much better when the assignment of correct
298 alleles are taken into account: the average number of correct alleles was 98.49%
299 (median = 99.67%), ranging from 92.12% (FGA) to 99.94% (D8S1179)
300 (Supplementary Table 3). The errors in allele assignment are summarized in
301 Supplementary Table 4. Inconsistencies were considered as “stutter-related”
302 errors when HipSTR failed to detect the smaller allele in situations in which the
303 CE-derived genotype indicated a heterozygote composed of contiguous alleles
304 (e.g., 11/12) and called it as a false homozygous (e.g., 12/12). Stutter-related
305 errors accounted for 13.2% of all errors. Other types of inconsistencies were
306 considered as “stutter-unrelated” errors (86.8%). All 311 errors are detailed in
307 Supplementary Table 5.

308 Allele frequencies estimated from the HGDP dataset were also compared
309 with STR data retrieved from the same seven major population groups that
310 composed the SPSmart STR browser (Amigo *et al.*, 2009) (Pop.STR) using F_{ST}
311 (Table 5). The Penta E marker presented values <0.05 in all groups except in the
312 Middle East (MES). In general, we observed only 10 significant F_{ST} spread out in
313 four markers: D2S441, D5S818, Penta D, and Penta E.

314 **Table 5. Probabilities obtained by F_{ST} analysis of population differentiation based on genotype frequencies of each STR, comparing**
 315 **population groups from the Human Genome Diversity Project with those from the SPSmart STR browser (Pop.STR). Significant p-values**
 316 **($\alpha = 0.05$) are in boldface. The probabilities that remain significant after the Bonferroni correction for multiple tests ($\alpha_{BONFERRONI} = 0.05/147$**
 317 **= 0.00034**) are also underlined.
 318

Marker	AFR		AMR		CSA		EAS		EUR		MES		OCE	
	F_{ST}	p-value												
CSF1PO	-0.00915	0.99980+-0.0001	-0.01250	0.85556+-0.0036	-0.00428	0.96010+-0.0021	-0.00433	0.99921+-0.0003	-0.00627	0.99584+-0.0006	-0.00614	0.99871+-0.0004	-0.02731	0.90872+-0.0032
D1S1656	-0.00938	0.99999+-0.0000	-0.01514	0.99994+-0.0000	-0.00492	0.99999+-0.0000	-0.00427	0.99998+-0.0000	-0.00616	0.99999+-0.0000	-0.00593	0.99999+-0.0000	-0.03287	0.99999+-0.0000
D2S441	-0.00905	0.99999+-0.0000	0.18667	<u>0.00000+-0.0000</u>	-0.00472	0.99792+-0.0001	-0.00412	0.99736+-0.0002	0.00523	0.11839+-0.0010	0.03174	<u>0.00063+-0.0001</u>	-0.03320	0.94017+-0.0008
D2S1338	0.00212	0.27614+-0.0014	-0.01342	0.97511+-0.0005	-0.00061	0.51765+-0.0017	0.00286	0.12064+-0.0010	0.00151	0.26167+-0.0014	-0.00443	0.96563+-0.0006	-0.03561	0.99999+-0.0000
D3S1358	-0.00958	0.99999+-0.0000	-0.01559	0.99697+-0.0002	-0.00480	0.99841+-0.0001	-0.00442	0.99999+-0.0000	-0.00627	0.99912+-0.0001	-0.00605	0.99853+-0.0001	-0.03566	0.99999+-0.0000
D5S818	-0.00902	0.99961+-0.0001	-0.01539	0.99631+-0.0002	-0.00496	0.99965+-0.0001	-0.00428	0.99908+-0.0001	-0.00644	0.99999+-0.0000	0.04888	<u>0.00000+-0.0000</u>	-0.03525	0.99999+-0.0000
D7S820	-0.00842	0.99382+-0.0002	-0.01511	0.99693+-0.0002	-0.00487	0.99962+-0.0001	-0.00443	0.99999+-0.0000	-0.00646	0.99999+-0.0000	-0.00570	0.99429+-0.0002	-0.02634	0.92461+-0.0008
D8S1179	-0.00953	0.99999+-0.0000	-0.01601	0.99999+-0.0000	-0.00500	0.99999+-0.0000	-0.00440	0.99999+-0.0000	-0.00632	0.99996+-0.0000	-0.00603	0.99995+-0.0000	-0.03535	0.99999+-0.0000
D10S1248	-0.00920	0.99997+-0.0000	-0.01472	0.99562+-0.0002	-0.00393	0.94223+-0.0007	-0.00385	0.97001+-0.0005	-0.00599	0.99106+-0.0003	-0.00569	0.99402+-0.0002	-0.03438	0.98741+-0.0003
D12S391	-0.00846	0.99995+-0.0000	-0.01439	0.99089+-0.0003	-0.00448	0.99985+-0.0000	-0.00247	0.84891+-0.0011	-0.00443	0.98000+-0.0004	-0.00459	0.98615+-0.0003	-0.03569	0.99999+-0.0000
D13S317	-0.00879	0.99329+-0.0003	-0.01328	0.96635+-0.0006	-0.00487	0.99981+-0.0000	-0.00432	0.99956+-0.0001	-0.00626	0.99988+-0.0000	-0.00605	0.99948+-0.0001	-0.03247	0.99041+-0.0003
D16S539	-0.00948	0.99992+-0.0000	-0.01540	0.99538+-0.0002	-0.00498	0.99999+-0.0000	-0.00418	0.99545+-0.0002	-0.00613	0.99891+-0.0001	-0.00616	0.99991+-0.0000	-0.03353	0.99790+-0.0001
D18S51	-0.00885	0.99994+-0.0000	-0.01508	0.99976+-0.0000	-0.00367	0.97798+-0.0005	-0.00281	0.91754+-0.0009	-0.00611	0.99997+-0.0000	-0.00585	0.99999+-0.0000	-0.01898	0.87383+-0.0010
D19S433	-0.00866	0.99983+-0.0000	-0.01513	0.99990+-0.0000	-0.00453	0.99955+-0.0001	-0.00324	0.93432+-0.0008	-0.00596	0.99906+-0.0001	-0.00596	0.99992+-0.0000	-0.03597	0.99999+-0.0000
D22S1045	0.00985	0.07334+-0.0008	-0.00716	0.55926+-0.0015	-0.00301	0.79675+-0.0013	-0.00370	0.95798+-0.0006	-0.00576	0.98184+-0.0004	-0.00513	0.97348+-0.0005	0.05184	0.06208+-0.0008
FGA	0.00366	0.19120+-0.0013	-0.01013	0.93542+-0.0008	-0.00156	0.67142+-0.0014	-0.00038	0.47693+-0.0016	-0.00438	0.94444+-0.0007	-0.00525	0.99428+-0.0003	-0.02768	0.99177+-0.0003
Penta D	0.02162	<u>0.00154+-0.0001</u>	-0.01285	0.94995+-0.0008	-0.00167	0.63971+-0.0015	-0.00248	0.83218+-0.0012	-0.00383	0.86665+-0.0011	-0.00469	0.97591+-0.0005	-0.02859	0.98105+-0.0004
Penta E	0.00953	<u>0.03937+-0.0006</u>	0.02947	<u>0.00501+-0.0002</u>	0.01702	<u>0.00010+-0.0000</u>	0.05375	<u>0.00000+-0.0000</u>	0.00603	<u>0.04632+-0.0007</u>	0.00332	0.13552+-0.0011	0.04362	<u>0.01032+-0.0003</u>
TH01	-0.00952	0.99999+-0.0000	-0.01577	0.99999+-0.0000	-0.00477	0.99722+-0.0002	-0.00437	0.99976+-0.0000	-0.00587	0.98292+-0.0004	-0.00551	0.98326+-0.0004	-0.03620	0.99999+-0.0000
TPOX	-0.00954	0.99987+-0.0000	-0.01540	0.99478+-0.0002	-0.00495	0.99929+-0.0001	-0.00432	0.99626+-0.0002	-0.00514	0.91091+-0.0009	-0.00617	0.99977+-0.0000	-0.03418	0.98061+-0.0004
vWA	-0.00788	0.98409+-0.0004	-0.01544	0.99814+-0.0001	-0.00498	0.99998+-0.0000	-0.00420	0.99766+-0.0001	-0.00590	0.99440+-0.0002	-0.00595	0.99843+-0.0001	-0.03169	0.99310+-0.0003

320 **DISCUSSION**

321
322 This study offers a STR database from high-coverage next-generation
323 sequencing data derived from the 54 population samples that compose the
324 Human Genome Diversity Project (HGDP).

325 Accurate STR genotyping from NGS data has been challenging due to the
326 high sequencing error rates and difficulties in aligning repetitive sequences
327 (Fungtammasan et al., 2015). However, Bornman et al. (2012) demonstrated that
328 CODIS *loci* could be accurately called even from complex mixtures using an NGS
329 approach. Notwithstanding that, capillary electrophoresis (CE) is, until now, and
330 will continue to be for a long time, the most used technique to genotype STRs
331 due to its simplicity. CE doesn't offer nucleotide sequence information (Bornman
332 et al., 2012), while an NGS assay allows differentiating isometric alleles
333 (isoalleles), which would permit to increase forensic informativeness (i.e., power
334 of discrimination and power of exclusion) (Hert et al., 2008). In this study, HipSTR
335 was used to differentiate alleles by size, and not by sequence due to the large
336 number of samples processed simultaneously.

337 HipSTR presented some problems in specific markers like D21S11, Penta D,
338 and Penta E. The D21S11 marker was excluded because HipSTR couldn't
339 genotype it. The same problem has already been reported by Valle-Silva et al.
340 (Valle-Silva et al., 2022) in a previous study. This could be related to the specific
341 region that HipSTR uses to capture this marker, given that D21S11 is a complex
342 marker (Rockenbauer et al., 2014). Moreover, the length of the sequenced alleles
343 may also play a part, given that even the smallest common D21S11 allele (with
344 26 repeats encompassing 104 nucleotides) is large, and sequencing error rates
345 increase with STR length (Kelkar et al., 2008). Both issues may lead to mapping
346 failure during the alignment step.

347 On the other hand, we may have failed in genotyping small Penta D alleles
348 that presented less than 5 repeats. This situation mainly affected the African
349 populations: many studies, including the pop.STR data (Amigo et al., 2009), show
350 that Penta D has a very high frequency of the 2.2 allele (0.20%). Also, in this
351 study Penta D presented the lowest successful calling rate (58.56%). Penta E
352 deviated from H-W equilibrium in 27 of 54 populations, being responsible for more
353 than 30% of Hardy-Weinberg departures observed. Because of these problems,

354 Penta D and Penta E were excluded from all interpopulation statistical analyses
355 (Analysis of Molecular Variance, PCoA and clustering analysis). We don't
356 recommend using these markers for population genetics or human identification
357 purposes using the HipSTR software. However, toaSTR (Carsten, 2017;
358 Ganschow et al., 2018; Valle-Silva; et al., 2022) showed very effective Penta D
359 and Penta E genotyping in previous studies. The limitation of this software, which
360 prevented its use in the present study, is that it can only process one sample at
361 a time, while HipSTR can process thousands of samples in parallel.

362 The D22S1045 marker showed to be monomorphic in an Amerindian
363 population from México, Pima. This population is considered to be composed of
364 descendants of the ancient Hohokam, who have inhabited the Sonoran Desert
365 and Sierra Madre regions for centuries. Today, they are present in two countries,
366 in the USA (Arizona state), as "*The O'odham*", and in Mexico as "*O'ob*" or "*Pima
367 Bajo*" (Schulz et al., 2015). According to the most recent data from the Mexican
368 government, currently, 1.540 Pima exist in the country (HOPE, 2006). The
369 SPSmart STR browser (Amigo et al., 2009) (Pop.STR) revealed precisely the
370 same situation, with only allele 15 being observed. The Pop.STR studied 14
371 individuals from this population, while HGDP sampled 13 individuals. Small
372 populations typically show a high rate of inbreeding, which produces the fixation
373 of some alleles (Hartl, 2020).

374 When the genotypes calculated with HipSTR were compared with those
375 from the dataset provided by Algee-Hewitt et al. (2016) and Rosenberg et al.
376 (2005), the average number of identical genotypes was 97.44% (median =
377 99.35%). The FGA and D22S1045 STRs were the most problematic ones and
378 strongly influenced the average. In the case of FGA, one of the reasons may be
379 the length of some alleles. For instance, although alleles with more than 30
380 repeats are extremely rare, the largest described FGA allele is composed of 51
381 tetranucleotide repeats. The observed stutter-unrelated problems could be
382 related to the positioning of flanking regions, tri-allelic patterns or alignment
383 errors. Although it is not reasonable to assign all the inconsistencies to problems
384 in the NGS-based procedure, particularly given that in the two CE-based studies
385 mentioned above were in fact large-scale genome-wide studies that prevented a
386 careful evaluation of each genotype for 1160 STRs in 2034 subjects from
387 worldwide populations, it is noteworthy that HipSTR uses previously obtained

388 bam files. Thus, additional efforts in improving the WGS alignment procedure,
389 particularly considering the repetitive nature of microsatellite regions, may
390 increase the overall accuracy of genotype calling by the HipSTR algorithm.
391 Unfortunately, CE-derived genotypes were unavailable for five markers
392 (D1S1656, D2S1338, D12S391, Penta D, and Penta E), rendering the secondary
393 validation attempt involving the comparison of allele frequencies using pairwise
394 F_{ST} of utmost importance to assess the reliability of their NGS-based genotypes.

395 The Principal Coordinates Analysis (PCoA) was able to separate the major
396 populations correctly (Figure 1) and also the sub-populations (Figure 2). Similar
397 results were revealed by the clustering analysis (Figure 3). While African,
398 Amerindian and Oceanian populations are clearly differentiated, Asian (CSA,
399 EAS, MES) and European (EUR) populations present high levels of shared
400 ancestry. Although modern humans arose in Africa, the Middle East is considered
401 the cradle of Eurasian civilization (Guest; Sahebkar, 2021), where the world's first
402 civilizations originated. Thanks to its economic supremacy, Europe ended up
403 colonizing the Middle East and leaving a large immigrant community. This
404 situation could be the reason for the genetic similarity between the individuals
405 from these regions. Historically, Central Asia has been an intersection between
406 Western and Eastern Eurasian people, leading to the current high levels of
407 genetic admixture and diversity (González-Ruiz et al., 2012).

408 The Structure analysis (Figure 3) shows that the African and Native American
409 populations form largely distinct homogeneous clusters, while the Middle
410 Eastern, European, Central, and South Asian populations form a more
411 heterogeneous cluster. These findings reflect the more isolated nature of the
412 former populations and corroborate the idea that although forensic STRs do show
413 relatively low F_{ST} , their high heterozygosities strengthens their capacity to
414 uncover patterns of population clustering, also revealed by other sets of markers
415 (JOBLING, 2022). Our findings agree with the data presented by Pemberton et
416 al. regarding human microsatellite variation on large databases, including the
417 HGDP-CEPH (Pemberton et al., 2013).

418 Despite the problems already discussed, HipSTR proved to be highly effective
419 for genotyping STR markers from NGS data, mainly for CODIS markers which
420 are the most used in the forensic area. Notwithstanding, we recommend using

421 more than one software to genotype these markers from NGS to obtain high
422 efficiency and circumvent the genotype calling issues we have described.

423

424 CONCLUSION

425

426 In conclusion, this investigation offers a population genetics perspective
427 based on a comprehensive genotyping analysis of standard STR used in the
428 forensic genetics field concerning the whole Human Genome Diversity Project.
429 Penta D and Penta D Markers were excluded from our analysis because they did
430 not show up as reliable markers. All the remaining genotypes and allele
431 frequencies presented in this study are supported by (a) previous reports that
432 certify HipSTR's reliability, (b) the comparison between CE-derived and NGS-
433 derived genotypes, (c) frequency data reports from worldwide populations,
434 including the large pop.STR database, and (d) the conclusions achieved by our
435 population genetics analysis that corroborates current knowledge regarding
436 modern human demographic history.

437

438 FUNDING

439

440 This study was financed in part by the Coordenação de Aperfeiçoamento de
441 Pessoal de Nível Superior - Brasil (CAPES) - Finance Code 001. C.T.M.J.
442 (#312802/2018-8) is supported by a Research Fellowship from CNPq/Brazil.

443

444 CONFLICTS OF INTEREST

445

446 The authors declare that there are no conflicts of interest.

447

448 COMPLIANCE WITH ETHICAL STANDARDS

449

450 Not applicable.

451

452 REFERENCES

453 Algee-Hewitt, B. F.; Edge, M. D.; Kim, J.; Li, J. Z. et al (2016). Individual
454 Identifiability Predicts Population Identifiability in Forensic Microsatellite
455 Markers. *Curr Biol* 26(7):935-942. Doi: 10.1016/j.cub.2016.01.065

456 Almarri MA, Bergström A, Prado-Martinez J, Yang F., et al (2020). Population
457 Structure, Stratification, and Introgression of Human Structural Variation. *Cell*.
458 9;182(1):189-199. Doi: 10.1016/j.cell.2020.05.024.

- 459 Amigo J.; Christopher, P.; Toño, S.; Fernandez, F.L., et al (2009). popSTR—An
460 online population frequency browser for established and new forensic STRs.
461 *Forensic Sci. Int. Genet. Suppl. Ser.* 2, 361–362. Doi:
462 10.1016/j.fsigss.2009.08.178
- 463 Behjati S, Tarpey PS (2013). What is next generation sequencing? *Arch Dis Child Educ Pract* 98(6):236-8. Doi: 10.1136/archdischild-2013-304340.
- 465 Bergström A, McCarthy SA, Hui R, Almarri MA., et al (2020). Insights into human
466 genetic variation and population history from 929 diverse genomes. *Science*
467 20;367(6484). Doi: 10.1126/science.aay5012
- 468 Birney E (2021). The International Human Genome Project. *Hum Mol Genet.*
469 1,30(R2):R161-R163. Doi: 10.1093/hmg/ddab198.
- 470 Bonneville R, Krook MA, Chen HZ, Smith A., et al (2020). Detection of
471 Microsatellite Instability Biomarkers via Next-Generation Sequencing.
472 *Methods Mol Biol.* 2055:119-132. Doi: 10.1007/978-1-4939-9773-2_5.
- 473 Bornman, D.M, Hester, M.E., Schuetter, J.M.; Kasoji, M.D., et al (2012). Short-
474 read, high-throughput sequencing technology for STR genotyping. *Biotech.*
475 *Rapid Dispatches* 1–6. Available at:
476 <https://www.ncbi.nlm.nih.gov/pmc/articles/PMC4301848/>
- 477 Callaway E (2019). First portrait of mysterious Denisovans drawn from DNA.
478 *Nature* 573(7775):475-476. Doi: 10.1038/d41586-019-02820-0.
- 479 Cann HM, de Toma C, Cazes L, Legrand MF., et al (2002) A human genome
480 diversity cell line panel. *Science* 12;296(5566):261-2. Doi:
481 10.1126/science.296.5566.261b.
- 482 Cavalli-Sforza LL (2005). The Human Genome Diversity Project: past, present
483 and future. *Nat Rev Genet.* 6(4):333-40. Doi: 10.1038/nrg1596.
- 484 Degioanni A, Bonenfant C, Cabut S, Condemi S (2019). Living on the edge: Was
485 demographic weakness the cause of Neanderthal demise? *PLoS One*
486 29;14(5):e0216742. Doi: 10.1371/journal.pone.0216742.
- 487 Demeter, F.; Zanolli, C.; Westaway, K. E.; Joannes-Boyau, R. et al (2022). A
488 Middle Pleistocene Denisovan molar from the Annamite Chain of northern
489 Laos. *Nat Commun.* 13(1):2557.
- 490 Dodson M, Williamson R (1999). Indigenous peoples and the morality of the
491 Human Genome Diversity Project. *J Med Ethics* 25(2):204-8. Doi:
492 10.1136/jme.25.2.204.
- 493 Excoffier, L.; Lischer, H.E (2010). Arlequin suite ver 3.5: A new series of programs
494 to perform population genetics analyses under Linux and Windows. *Mol. Ecol.*
495 *Resour.* 10, 564–567. Doi: 10.1111/j.1755-0998.2010.02847.x
- 496 Fan H, Chu JY (2007). A brief review of short tandem repeat mutation. *Genomics*
497 *Proteomics Bioinformatics* 5(1):7-14. Doi: 10.1016/S1672-0229(07)60009-6.

- 498 Fungtammasan, A.; Ananda, G.; Hile, S.E.; Su, M.S., et al (2015). Accurate typing
499 of short tandem repeats from genome-wide sequencing data and its
500 applications. *Genome Res.* 25, 736–749. Doi: 10.1101/gr.185892.114.
- 501 Ganschow, S.; Silvery, J.; Kalinowski, J.; Tiemann, C (2018). toaSTR: A web
502 application for forensic STR genotyping by massively parallel sequencing.
503 *Forensic Sci. Int. Genet.* 37, 21–28. Doi: 10.1016/j.fsigen.2018.07.006.
- 504 Gettings, K.B.; Ballard, D.; Bodner, M.; Borsuk, L.A., et al (2019). Report from
505 the STRAND Working Group on the 2019 STR sequence nomenclature
506 meeting. *Forensic Sci. Int. Genet.* 43, 102165. Doi:
507 10.1016/j.fsigen.2019.102165.
- 508 González-Ruiz M, Santos C, Jordana X, Simón M., et al (2012). Tracing the origin
509 of the east-west population admixture in the Altai region (Central Asia). *PLoS*
510 One 7(11):e48904. Doi: 10.1371/journal.pone.0048904.
- 511 Gouy, A.; Zieger, M (2017). STRAF-A convenient online tool for STR data
512 evaluation in forensic genetics. *Forensic Sci. Int. Genet.* 30, 148–151. Doi:
513 10.1016/j.fsigen.2017.07.007.
- 514 Guest PC, Sahebkar A (2021). Research in the Middle East into the Health
515 Benefits of Curcumin. *Adv Exp Med Biol.* 1291:1-13. Doi: 10.1007/978-3-030-
516 56153-6_1.
- 517 Gymrek, M.; Golan, D.; Rosset, S.; Erlich, Y (2012). lobSTR: A short tandem
518 repeat profiler for personal genomes. *Genome Res.* 22, 1154–1162. Doi:
519 10.1101/gr.135780.111.
- 520 Halman, A.; Oshlack, A (2020). Accuracy of short tandem repeats genotyping
521 tools in whole exome sequencing data. *F1000Res* 9, 200. Doi:
522 10.12688/f1000research.22639.1
- 523 Hartl, D (2020). A Primer of Population Genetics and Genomics. 4a ed. Oxford
524 University Press.
- 525 Hert DG, Fredlake CP, Barron AE (2008). Advantages and limitations of next-
526 generation sequencing technologies: a comparison of electrophoresis and
527 non-electrophoresis methods. *Electrophoresis* 29(23):4618-26. Doi:
528 10.1002/elps.200800456.
- 529 Hope, M (2006). Pueblos Indígenas del México Contemporáneo. 2006. Available
530 from: <https://www.inpi.gob.mx/2021/dmdocuments/pimas.pdf>.
- 531 Hubisz MJ, Falush D, Stephens M, Pritchard JK (2009). Inferring weak population
532 structure with the assistance of sample group information. *Mol Ecol Resour*
533 9(5):1322-32. Doi: 10.1111/j.1755-0998.2009.02591.x.
- 534 Jobling, M.A (2022). Forensic genetics through the lens of Lewontin: Population
535 structure, ancestry and race. *Philos. Trans. R. Soc. Lond. B Biol. Sci.* 2022,
536 377, 20200422. Doi: 10.1098/rstb.2020.0422

- 537 Kelkar YD, Tyekucheva S, Chiaromonte F, Makova KD (2008). The genome-wide
538 determinants of human and chimpanzee microsatellite evolution. *Genome Res*
539 18(1):30-8. Doi: 10.1101/gr.7113408.
- 540 Kopelman NM, Mayzel J, Jakobsson M, Rosenberg NA., et al (2015). Clumpak:
541 a program for identifying clustering modes and packaging population structure
542 inferences across K. *Mol Ecol Resour* 15(5):1179-91. doi: 10.1111/1755-
543 0998.12387.
- 544 Mallick S, Li H, Lipson M, Mathieson I., et al (2016). The Simons Genome
545 Diversity Project: 300 genomes from 142 diverse populations. *Nature*
546 13;538(7624):201-206. Doi: 10.1038/nature18964.
- 547 Peakall, R.; Smouse, P.E (2012). GenAIEx 6.5: Genetic analysis in Excel.
548 Population genetic software for teaching and research-an update.
549 *Bioinformatics* 28, 2537–2539. Doi: 10.1093/bioinformatics/bts460
- 550 Pemberton TJ, DeGiorgio M, Rosenberg NA (2013). Population structure in a
551 comprehensive genomic data set on human microsatellite variation. *G3*
552 Bethesda 20;3(5):891-907. Doi: 10.1534/g3.113.005728
- 553 Robinson, J.T.; Thorvaldsdóttir, H.; Wenger, A.M.; Zehir, A., et al (2017). Variant
554 Review with the Integrative Genomics Viewer. *Cancer Res.* 77, e31–e34. Doi:
555 10.1158/0008-5472.CAN-17-0337
- 556 Rockenbauer E, Hansen S, Mikkelsen M, Børsting C., et al (2014).
557 Characterization of mutations and sequence variants in the D21S11 locus by
558 next generation sequencing. *Forensic Sci Int Genet* 8(1):68-72. Doi:
559 10.1016/j.fsigen.2013.06.011.
- 560 Rosenberg NA (2006). Standardized subsets of the HGDP-CEPH Human
561 Genome Diversity Cell Line Panel, accounting for atypical and duplicated
562 samples and pairs of close relatives. *Ann Hum Genet.* 70(Pt 6):841-7. Doi:
563 10.1111/j.1469-1809.2006.00285.x.
- 564 Rosenberg NA, Mahajan S, Ramachandran S, Zhao C., et al (2005). Clines,
565 clusters, and the effect of study design on the inference of human population
566 structure. *PLoS Genet* 1(6):e70. Doi: 10.1371/journal.pgen.0010070.
- 567 Schulz LO, Chaudhari LS (2015). High-Risk Populations: The Pimas of Arizona
568 and Mexico. *Curr Obes Rep.* 4(1):92-8. Doi: 10.1007/s13679-014-0132-9
- 569 Thorvaldsdóttir, H.; Robinson, J.T.; Mesirov, J.P (2013). Integrative Genomics
570 Viewer (IGV): High-performance genomics data visualization and exploration.
571 *Brief. Bioinform.* 14, 178–192. Doi: 10.1093/bib/bbs017.
- 572 Valle-Silva, G.; Frontanilla, T.S.; Ayala, J.; Donadi, E.A., et al (2022). Analysis
573 and comparison of the STR genotypes called with HipSTR, STRait Razor and
574 toaSTR by using next generation sequencing data in a Brazilian population
575 sample. *Forensic Sci. Int. Genet.* 58, 102676. Doi:
576 10.1016/j.fsigen.2022.102676

577 Warshauer, D.H.; Lin, D.; Hari, K.; Jain, R., et al (2013). STRait Razor: A length-
578 based forensic STR allele-calling tool for use with second generation
579 sequencing data. *Forensic Sci. Int. Genet.* 7, 409–417. Doi:
580 10.1016/j.fsigen.2013.04.005

581 Willems, T.; Zielinski, D.; Yuan, J.; Gordon, A., et al (2017). Genome-wide
582 profiling of heritable and de novo STR variations. *Nat. Methods* 14, 590–592.
583 Doi: 10.1038/nmeth.4267

584

585